

The quiescent light curve and evolutionary state of GRO J1655–40

Martin E. Beer^{*} and Philipp Podsiadlowski

University of Oxford, Nuclear and Astrophysics Laboratory, Oxford, OX1 3RH, England

25 October 2018

ABSTRACT

We present ellipsoidal light-curve fits to the quiescent B , V , R and I light curves of GRO J1655–40 (Nova Scorpii 1994). The fits are based on a simple model consisting of a Roche-lobe filling secondary and an accretion disc around the black-hole primary. Unlike previous studies, no assumptions are made about the interstellar extinction or the distance to the source; instead these are determined self-consistently from the observed light curves. In order to obtain tighter limits on the model parameters, we used the distance determination from the kinematics of the radio jet as an additional constraint. We obtain a value for the extinction that is lower than was assumed previously; this leads to lower masses for both the black hole and the secondary star of $5.4 \pm 0.3 M_{\odot}$ and $1.45 \pm 0.35 M_{\odot}$, respectively. The errors in the determination of the model parameters are dominated by systematic errors, in particular due to uncertainties in the modeling of the disk structure and uncertainties in the atmosphere model for the chemically anomalous secondary in the system. A lower mass of the secondary naturally explains the transient nature of the system if it is either in a late case A or early case B mass-transfer phase.

Key words: accretion, accretion discs - stars: individual: GRO J1655–40 - binaries: close - X-rays: stars.

1 INTRODUCTION

GRO J1655–40 is a well studied soft X-ray transient (SXT) with an orbital period of 2.62168 ± 0.00014 d (van der Hooft et al. 1997, hereafter vdH). It contains a F3–5 giant or sub-giant with an effective temperature of approximately 6500 K (Orosz & Bailyn 1997, hereafter OB). Shahbaz et al. 1999 (hereafter S99) obtained the radial-velocity curve of the system during quiescence using high-resolution spectroscopy and found a mass function of $2.73 \pm 0.09 M_{\odot}$. This value is significantly lower than the previous estimates by Bailyn et al. (1995b, $3.16 \pm 0.15 M_{\odot}$) and OB ($3.24 \pm 0.09 M_{\odot}$), most likely because their radial-velocity determination relied on some data that were obtained during outburst (see Phillips, Shahbaz & Podsiadlowski 1999). From the rotational broadening of the spectral lines, they also obtained a constraint on the mass ratio of 2.29–3.06.

In their original study, OB modelled the ellipsoidal light curve during quiescence assuming a polar temperature of 6500 K for the secondary and found an inclination of $69^{\circ}.50 \pm 0^{\circ}.08$ and a mass ratio of 2.99 ± 0.08 . These values imply masses of $7.02 \pm 0.22 M_{\odot}$ and $2.34 \pm 0.12 M_{\odot}$ for the black hole and secondary star, respectively. VdH also modelled

the ellipsoidal light curve during quiescence and obtained an inclination of $63^{\circ}.7 - 70^{\circ}.7$ and a secondary mass in the range of $1.60 - 3.10 M_{\odot}$, which implies a mass ratio of 2.43–3.99.

VdH’s estimates have larger uncertainties since, unlike OB, they considered models with three different luminosities (31 , 41 and $54 L_{\odot}$) taking into account uncertainties in the distance (3.2 ± 0.2 kpc, obtained from the kinematics of the observed radio jet; Hjellming & Rupen 1995) and in the colour excess ($E(B - V) = 1.3 \pm 0.1$, based on various previous estimates; see vdH). Combining a value for $E(B - V)$ of 1.3 with the observed $B - V$ colour of approximately 1.55 implies an intrinsic $(B - V)_0$ of less than 0.25 (this is an upper limit, since any disc contribution tends to be redder than this). A $(B - V)_0$ of less than 0.25 corresponds to a sub-giant of spectral type A8 or earlier (Fitzgerald 1970) whilst the $(B - V)_0$ of a F3–5 giant or sub-giant is 0.39–0.44. This immediately demonstrates that a value for $E(B - V)$ of 1.3 is not consistent with the observed spectral type. An overestimate of $E(B - V)$ leads to an overestimate of the bolometric luminosity of the secondary, which in turn requires a larger and more massive secondary. More recent estimates of the ultraviolet extinction (Hynes et al. 1998) yielded an $E(B - V)$ of 1.2 ± 0.1 . This implies a secondary of lower luminosity than considered by vdH.

^{*} E-mail: beer@astro.ox.ac.uk

Both OB and vdH allowed an arbitrary magnitude offset for each passband (B , V , R , I) when they modelled the ellipsoidal light curves. This has the same effect as allowing the distance and the colour excess to vary independently for different passbands. It also means that they were not using all the available information. In particular, this did not allow them to check whether their best-fitting models were actually consistent with the observed spectral type.

In the present study we avoid these problems by fitting the ellipsoidal light curves for all passbands simultaneously (without arbitrary offsets), but allowing the distance and the colour excess to vary freely. As a consequence, the distance and the colour excess are determined self-consistently from the best-fitting models instead of being taken as input parameters.

In Section 2 we outline the basic model used in this study. In Section 3 we apply it to fit the quiescent light-curve data of OB for different disc structures and obtain a new model for all parameters of GRO J1655–40 and examine their uncertainties. In Section 4 we show how the variation in temperature across the surface of the secondary limits the accuracy to which the spectral type of the secondary can be determined. Finally, in Section 5 we compare our results to previous studies and discuss the implications of our new model for the evolutionary state of the system.

2 DESCRIPTION OF THE MODEL

Our method to model the ellipsoidal light curve of Nova Sco is similar in many respects to the methods used previously by OB and vdH. It consists of a Roche-lobe filling secondary and a simple model for the accretion disc.

For a given value of the polar temperature, the temperature across the secondary is determined using a standard linear limb-darkening law, where the coefficients for each surface element are calculated by interpolating the tables of Wade & Rucinski (1985).

Similar to OB and vdH, we model the accretion disc as a flat cylindrical disc with an opening angle of 2° . For the inner disc radius we follow OB and take, at least initially, a small value of 0.005 of the effective Roche-lobe radius (r_L). We varied the outer disc radius, which is limited by the tidal disruption radius, considering outer disc radii of 0.7, 0.8 and 0.9 r_L , respectively. For the temperature profile we adopted a simple power-law profile, $T_{\text{disc}} \propto r^\alpha$, where we considered both a flat temperature profile with $\alpha = -0.1$ and a standard steady-disc profile with $\alpha = -0.75$ (Shakura & Sunyaev 1973). The constant of proportionality in the temperature power-law profile depends on both the outer disc temperature and the outer disc radius. In order to make the temperature structure independent of r_{out} , we scaled the disc rim temperature to correspond to the same temperature at $r = 0.9 r_L$ (i.e. discs with different outer radii will all have the same temperature at $r = 0.7 r_L$).

To model the emission from the secondary and the disc, we divide the secondary and the surface of the accretion disc into discrete elements and determine the local gravity and temperature for each element. Unlike previous studies, we do not assume that the emission on the secondary is that of a blackbody; instead we calculate it from the model atmospheres by Kurucz (1992). For this purpose, we have

constructed a table, which gives the emission in different passbands (B , V , R , I) as a function of temperature, surface gravity and $E(B - V)$. To calculate the emission, we first corrected the Kurucz model atmospheres for interstellar extinction for a specified value of $E(B - V)$ using a mean Galactic extinction curve (Fitzpatrick 1999) and calculated the extinction at each wavelength. It is important to correct for the extinction first since there is a large variation in extinction across the broadband passbands: for example in the V band, $E(\lambda - V)/E(B - V)$ varies from 3.8 to 2.1. We then folded the extinction-corrected atmospheres through standard filter response curves (Bessell 1990) to obtain the emission in each passband. Standard Vega fluxes (Tüg, White & Lockwood 1977) were used to calculate the zero point corrections to the magnitudes. The emission from the disc was calculated similarly except that extinction-corrected blackbody spectra were folded through the passbands rather than model atmospheres. Recently Greene, Baily & Orosz (2001) have also modelled the ellipsoidal light curves using model atmosphere fluxes and their analysis is discussed further in Section 3.3.3.

The model atmospheres we used in this analysis were of solar abundance. The metal abundances of the secondary in GRO J1655–40 have been measured by Israelian et al. (1999) who found $[\text{Fe}/\text{H}] = 0.1 \pm 0.2$, but with an overabundance of α -elements compared to solar values. Their α -element abundances are $[\text{O}/\text{H}] = 1.0 \pm 0.3$, $[\text{S}/\text{H}] = 0.75 \pm 0.2$, $[\text{Mg}/\text{H}] = 0.9 \pm 0.40$, $[\text{Si}/\text{H}] = 0.9 \pm 0.3$, $[\text{Ti}/\text{H}] = 0.9 \pm 0.4$ and $[\text{N}/\text{H}] = 0.45 \pm 0.5$. A solar Fe abundance is supported by Buxton & Vennes (2001) who find $[\text{Fe}/\text{H}] = -0.25 - 0.00$. As detailed α -element-enhanced model atmospheres are not freely available we are unable to use α -element-enhanced model atmospheres in our calculations. The majority of the spectral lines, however, are due to Fe and so the use of the correct Fe abundance is the most important factor in choosing the metallicity and reassures us that this is the correct metallicity to choose.

In Fig. 1 we demonstrate how important it is to use model atmospheres rather than blackbody spectra. It shows the difference between a 6500 K blackbody and a model atmosphere of the same temperature with a gravity of 3.0 dex. This temperature corresponds to a star with a spectral type similar to GRO J1655–40. The spectra are significantly different, especially in the B band region. For the I band region, the model atmosphere is similar to the Rayleigh-Jeans tail of a blackbody; hence the blackbody assumption would be valid in this passband. Orosz & Hauschildt (2000) have investigated the difference between blackbodies and model atmosphere calculations and found that, with the inclusion of model atmospheres, the minima of the light curve tend to be deeper for the visible and infrared passbands, since at the minima the coolest parts of the secondary are visible (e.g. the L1 point at phase 0.5) and for cool temperatures the differences between model atmospheres and blackbodies are largest.

For a particular disc model, our ellipsoidal light-curve model has five free model parameters: the mass ratio, system inclination, colour excess, distance to Nova Sco and polar temperature (T_{pole}) of the secondary star. The individual component masses (M_1 and M_2) are calculated from the mass function, where we use the value of $2.73 \pm 0.09 M_\odot$ (S99). We determine these five free parameters by compar-

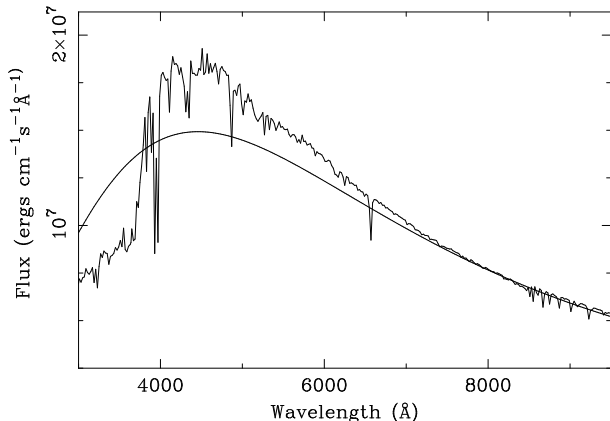


Figure 1. The difference in spectra between a 6500 K blackbody and a model atmosphere of the same temperature and a gravity of 3.0 dex.

ing our model ellipsoidal light curves to the quiescent B , V , R and I band data (OB), kindly provided by J. A. Orosz, using a standard chi-squared test. The quiescent data are much better sampled in the V and I bands than the in B and R bands (there are 6-7 times as many data points in V and I compared to B and R). This has the consequence of giving more weight to the V and I data points and hence produces a better fit in these passbands than in B and R . OB tried to compensate for this by giving each point in the B and R passbands seven times the weight in their fitting procedure than in the other passbands. However, this gives too much weight to any outlying points the data contains as the number of ~ 25 points in each of these two passbands is not large enough to eliminate small number statistical effects (e.g. the different R magnitudes at phases 0.25 and 0.75 of the data cannot be modelled properly). We therefore chose to give each point equal weight. A grid search was used to find the best-fitting model as this is the most reliable way of finding the global minimum. Since the measurement errors are not normally distributed, it is not valid to establish quantitative relationships between $\Delta\chi^2$ and the confidence limits. The χ^2 test therefore provides a merit function not a maximum likelihood estimator. Because of this, the Hessian matrix (the inverse of the covariance matrix) was not used for error estimation, but a constant $\Delta\chi^2$ was chosen as the boundary to define confidence regions.

The parameters of the model are highly correlated with each other. For example, an increase in distance (which makes the object fainter) can be compensated, at least to some degree, in several different ways: (1) by a decrease in mass ratio, which increases the secondary’s Roche-lobe radius and hence increases its surface area; (2) a decrease in $E(B - V)$, which reduces the extinction; or (3) an increase in temperature, which makes the object more luminous. The distance to Nova Sco is relatively well determined from the kinematics of the radio jet (Hjellming & Rupen 1995), and we use this as an additional constraint in the modelling, in order to obtain tighter limits on the various model parameters. The colour excess and temperature of the secondary can be used to estimate the spectral type. This allows us to check whether the best-fitting parameters are consistent with the observed spectral type of Nova Sco. This is prefer-

able to the previous analyses, which allowed an arbitrary shift in the light curves, thereby losing information on the distance and extinction. Shifting the light curves also has the effect of making the light-curve amplitudes strongly dependent on the proportion of disc flux. The present method avoids this problem as altering the proportion of disc flux shifts the light curves while also altering their amplitudes. Therefore, an overestimate of the disc flux will be seen as a shift in the light curves toward brighter magnitudes. If the light curves were arbitrarily offset, this would only appear as a change in amplitude which could be compensated by a change in inclination, mass ratio or temperature.

The treatment of the distance and the colour excess as free parameters, and the inclusion of model atmosphere fluxes, are the only significant differences between our model and those of OB and vdH. Indeed, we have checked that, using the same assumptions as OB and vdH, we obtain light-curve fits that are essentially identical to those in these respective studies.

3 LIGHT-CURVE MODELLING

3.1 The disc structure

In our initial modelling we assumed a steady-state disc where the temperature profile follows a $-3/4$ power law (i.e. $T_{\text{disc}} \propto r^{-3/4}$). This corresponds to an optically thick disc where each element emits like a blackbody (Shakura & Sunyaev 1973). In such a disc, most of the contribution to the observed disc flux comes from the inner parts of the disc. We systematically varied the temperature at the disc rim, but did not find any model that produced a good fit to the observed light curves since all models produced too much blue light in the inner parts of the disc. The best fit was obtained for a cool accretion disc with a rim temperature of 1000 K, which had a $\chi^2_{\nu, \text{min}}$ of 2.1. However, in this model the fitted distance was much closer than the distance of 3.2 ± 0.2 kpc found by Hjellming & Rupen (1995); hence this model also had to be discarded.

We then considered two alternative types of disc model: (1) an accretion disc with a central hole and (2) a disc with a flat temperature profile.

A central hole in the accretion disc of GRO J1655–40 has previously been proposed by Hameury et al. (1997) to explain the time delay between the optical and the X-ray outbursts. Models for discs with central holes have also been suggested by various authors for a variety of systems (e.g. Meyer & Meyer-Hofmeister 1994; Meyer-Hofmeister & Meyer 2000; Narayan, McClintock & Yi 1996). In these models the hole is caused by evaporation of the inner parts of the disc. Here, we assumed that the temperature at the inner edge of the disc did not exceed 7000 K (a higher temperature would produce too much blue light). The 7000 K cutoff corresponds to $r = 0.067 r_L$ and $r = 0.17 r_L$ for rim temperatures of 1000 and 2000 K, respectively.

In cataclysmic variables (CVs), maximum entropy eclipse mapping (MEM) has been used to determine the radial temperature profile of the discs (Horne 1993). In outburst, the disc temperature profile is generally found to be consistent with a $-3/4$ power law, whilst in quiescence the profile is significantly less steep, occasionally even flat

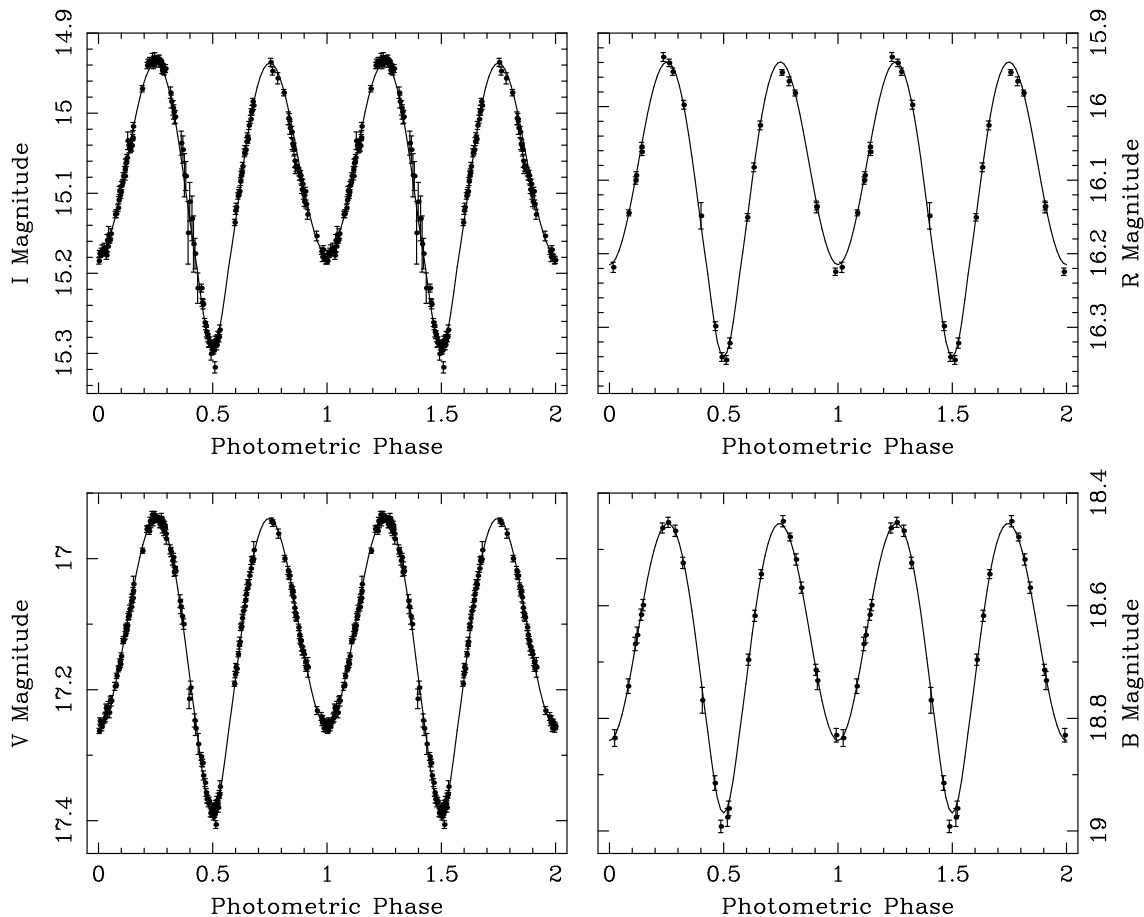


Figure 2. Fits to the data for the best-fitting parameters.

(Wood et al. 1986, 1989). It has been suggested that the temperature profile in SXTs will also be flat during quiescence (Janet Wood, private communication). In their study, OB let the power-law index of the disc temperature profile be a free parameter and found a value of -0.12 for their best-fitting model. Based on this finding, we adopted a power-law index of -0.1 for our model with a flat temperature profile. Since for such a profile, most of the flux comes from the outer parts of the disc, this model is not sensitive to the chosen inner disc radius.

In models with a disc rim temperature of 1000 K, the disc does not contribute much flux to the system. Its principle effect is in eclipsing the secondary and thereby increasing the depth of the minimum at phase 0.5. Therefore, the addition of a central hole did not improve the fit. The best-fitting model for the disc with the central hole was obtained for a rim temperature of 2000 K. This model has a reduced $\chi^2_{\nu, \min}$ of 1.7 for 370 degrees of freedom. The 2000 K disc contributes a greater proportion of the system's flux than the cooler 1000 K disc. The disc with the flat temperature profile was modelled so that it produced the same amount of flux as the 2000 K disc with the central hole (~ 5 per cent in V). This corresponds to a rim temperature of 3500 K at $0.9 r_L$. This model produced the overall best fit with a $\chi^2_{\nu, \min}$ of 1.65.

To improve the fits further, we then used a finer grid with spacings of 0.1 in the mass ratio, 0.1° in inclination,

0.001 in $E(B - V)$, 0.002 kpc in distance and 25 K in polar temperature for the two disc models. The results of the best fits are shown in Table 1 for the two types of disc models. The light-curve fits for the best-fitting model with a flat disc profile and outer disc radius of $0.8 r_L$ are shown in Fig. 2 (this model has a reduced $\chi^2_{\nu, \min}$ of 1.614).

3.2 Confidence limits for the system parameters

The fitting procedure has two sources of errors: one is the general statistical error and the other is caused by the finite size of the grid. Ideally, an iterative process would be used to find the global minimum at each value of a parameter. However, we found that there were a large number of minima and that an iterative process was not guaranteed to find the global minimum. To estimate the effect of the finite grid size, we used the following procedure. At the minimum we estimated the effect of the finite grid size on each parameter in turn by fixing that parameter to the value it has at the minimum and by varying the other parameters systematically. For each parameter we calculated the increase in χ^2 corresponding to a value half a grid spacing away. The largest increase in the value of χ^2 was then taken as the uncertainty, $\Delta\chi^2$, in χ^2 due to the grid resolution for the particular parameter kept fixed. The 90 per cent confidence limits generally generate an increase in χ^2 of 2.71 (Avni 1976). We added this to $\Delta\chi^2$ and used the resulting value

Table 1. Best-fitting parameters for models with a flat disc temperature profile and for a steady-state disc with an inner disc temperature of 7000 K and disc rim temperature of 2000 K.

Parameter	Model					
	$r_{\text{out}}/r_{\text{L}}$ for $T_{\text{disc}} \propto r^{-0.1}$			$r_{\text{out}}/r_{\text{L}}$ for $T_{\text{in}} = 7000$ K		
	0.7	0.8	0.9	0.7	0.8	0.9
Mass ratio	3.4	3.9	4.0	3.9	4.4	5.3
Inclination	69°5	68°4	67°3	70°0	68°7	67°4
T_{pole} (K)	6625	6525	6350	6850	6750	6725
$E(B - V)$	1.037	1.001	0.950	1.089	1.067	1.055
Distance (kpc)	3.340	3.208	3.248	3.138	2.998	2.820
Minimum χ^2_{ν}	1.644	1.614	1.764	1.697	1.675	1.673
M_1 (M_{\odot})	5.65	5.35	5.45	5.20	5.10	4.90
M_2 (M_{\odot})	1.65	1.40	1.35	1.35	1.15	0.90
L_2 (L_{\odot})	25.0	20.5	18.5	24.5	21.0	17.5
T_{eff} (K)	6200	6100	5925	6450	6325	6325

Table 2. 90 per cent confidence limits for a steady-state disc with a central hole. The inner disc temperature of 7000 K corresponds to r_{in} of 0.17 r_{L} .

Parameter	Outer disk radius		
	0.7	0.8	0.9
Mass ratio	3.65 - 4.15	4.20 - 4.75	5.00 - 5.90
Inclination	69°75 - 70°15	68°50 - 68°90	67°20 - 67°65
T_{pole} (K)	6720 - 6935	6670 - 6875	6610 - 6785
$E(B - V)$	1.057 - 1.117	1.039 - 1.103	1.030 - 1.074
Distance (kpc)	2.995 - 3.296	2.890 - 3.096	2.685 - 2.912
M_1 (M_{\odot})	5.05 - 5.35	4.95 - 5.20	4.70 - 5.00
M_2 (M_{\odot})	1.20 - 1.45	1.05 - 1.25	0.80 - 1.00
L_2 (L_{\odot})	22.5 - 26.5	19.5 - 22.5	15.5 - 19.0
T_{eff} (K)	6250 - 6500	6225 - 6425	6150 - 6350

to define the 90 per cent confidence region and to obtain the confidence limits for each individual parameter.

The masses of the two binary component masses are not parameters that are fitted directly, but are determined from the mass function (kept fixed) and the values of the inclination and mass ratio at a particular grid-point in the five-dimensional model parameter space. To determine the uncertainty in χ^2 due to the finite grid size, we used a similar method as above, except that this time both the mass ratio and the inclination of the system were held fixed at their values at the minimum and the remaining three parameters were varied to find $\Delta\chi^2$. The 90 per cent confidence limits for a quantity depending on two parameters generates an increase in χ^2 of 4.61 (Avni 1976). This was added to $\Delta\chi^2$ and the result was used to define the confidence regions for the component masses. Similarly, to calculate the confidence limits for the luminosity (L_2) and effective temperature (T_{eff}) of the secondary, the same method was used, except that these quantities depend on three parameters: the mass ratio, the inclination and the polar temperature. The luminosity was calculated by summing σT^4 over the surface, and the effective temperature by dividing the luminosity by the surface area. The effect of the finite size of the grid in the distance and colour excess was then found and added to the increase in χ^2 , corresponding to the 90 per cent confidence

limits for a quantity depending on three parameters (6.25, Avni 1976).

The 90 per cent confidence limits for the steady-state disc models with a central hole with an inner edge disc temperature of 7000 K are shown in Table 2. This inner edge disc temperature corresponds to $r_{\text{in}} = 0.17 r_{\text{L}}$. Table 2 shows that, as the outer disc radius is increased in this model, the mass ratio increases and the distance decreases while the secondary temperature and luminosity remain the same. The secondary temperature and luminosity are consistent with the observed $B - V$, whilst only the outer disc radius of 0.7 r_{L} has a distance which is consistent with that of Hjellming & Rupen (1995). (The model with an outer disc radius of 0.8 r_{L} is marginally consistent.)

The 90 per cent confidence limits for the parameters and the derived quantities are shown in Table 3 for the disc model with a -0.1 temperature profile. Table 3 shows that, as the outer disc radius is increased in this model, the temperature of the secondary decreases, as does the colour excess. This is consistent as a lower temperature implies a later spectral type which has a larger $(B - V)_0$. The distances are similar to the measurement of Hjellming & Rupen (1995) for all values of the outer disc radius.

Comparison of the various models in Tables 2 and 3 shows that the variation in the parameters from model to

Table 3. 90 per cent confidence limits for a disc with a flat temperature profile.

Parameter	Outer disk radius		
	0.7	0.8	0.9
Mass ratio	3.30 - 3.60	3.55 - 4.00	3.65 - 4.50
Inclination	69°35 - 69°75	68°25 - 68°60	67°10 - 67°60
T_{pole} (K)	6550 - 6745	6380 - 6570	6210 - 6410
$E(B - V)$	1.017 - 1.067	0.970 - 1.019	0.917 - 0.962
Distance (kpc)	3.167 - 3.496	3.116 - 3.398	3.106 - 3.352
M_1 (M_{\odot})	5.35 - 5.70	5.30 - 5.60	5.15 - 5.70
M_2 (M_{\odot})	1.45 - 1.80	1.30 - 1.60	1.10 - 1.60
L_2 (L_{\odot})	22.5 - 27.0	19.0 - 23.0	15.0 - 20.5
T_{eff} (K)	6100 - 6300	5950 - 6150	5750 - 6025

Table 4. Best-fitting model parameters for Nova Sco

Mass ratio	3.9 ± 0.6
Inclination	$68^{\circ}65 \pm 1^{\circ}5$
T_{pole}	6575 ± 375 K
M_1	$5.40 \pm 0.30 M_{\odot}$
M_2	$1.45 \pm 0.35 M_{\odot}$
L_2	$21.0 \pm 6.0 L_{\odot}$
T_{eff}	6150 ± 350 K
$E(B - V)$	1.0 ± 0.1

model is larger than the statistical errors for each individual model (as given in the tables) and that the systematic errors due to the uncertainties in the modelling are the dominant sources of error. We can use this variation of parameters as an *indication* of the systematic errors, although we need to emphasize that this is really only a lower limit, since we only examined a limited number of models. Using the distance measurement by Hjellming & Rupen (1995) as an additional discriminant, we obtain the best-guess estimates for the parameters given in Table 4 with uncertainties that include both the statistical errors and an estimate of the systematic errors.

3.3 Checking for self-consistency

3.3.1 The colour and spectral type of the secondary

To determine the intrinsic $(B - V)_0$ of the secondary, the contribution of the disc to the overall $B - V$ has to be subtracted. This was done by calculating the $B - V$ for the best-fitting models when the disc flux was not included. This resulted in a decrease in $B - V$ of 0.01–0.02. The $E(B - V)$ of the best-fitting models then leads to a $(B - V)_0$ of 0.42–0.61 for the secondary, which corresponds to a spectral-type range of F4–G0 (Fitzgerald 1970). This is a somewhat later spectral type than found in previous estimates but is consistent with the analysis using quiescent data (S99). The spectral type can also be determined from the effective temperature (6150 ± 350 K). This temperature range corresponds to the spectral-type range F5–G2 (Straizys & Kuriliene 1981). The two measurements are consistent with each other, implying a spectral type for the secondary of F5–G0. We note, however, that due to the highly anomalous chemical compo-

sition of the secondary (Israelian et al. 1999), it is not clear how well these standard relations apply.

In our model we have assumed that the temperature distribution of the secondary star is described by a gravity-darkening law appropriate for a radiative atmosphere (von Zeipel 1924), for which the local temperature is proportional to the local value of gravity to the 0.25 power. If the atmosphere were convective, we would expect a gravity-darkening coefficient of 0.08 (Lucy 1967). The deduced spectral type of the secondary (F5–G0) is on the boundary between hot stars with radiative atmospheres and cool stars with convective atmospheres. If the atmosphere were convective (with a coefficient of 0.08), then the temperature variation over the surface would be smaller than in the radiative case, and the system would require a higher inclination to give the same light-curve amplitude. However, a larger inclination would produce deeper, sharper eclipses which are not observed. This suggests that the steeper gravity-darkening coefficient for radiative atmospheres is indeed the most appropriate to use. Near the L1 point, the star’s temperature (~ 4000 K) is cooler than the polar temperature because of the lower surface gravity (2.5 vs. 3.5 dex). This implies that the L1 point may be convective rather than radiative. However, this would only affect the light curve near phase 0.5, when the accretion disc is in front of the secondary. Thus, any difference could be represented by a variation in the amount of eclipsing, i.e. the size of the disc. As we have considered three different disc sizes, we can be confident that this effect does not significantly add to the uncertainties.

Unlike the previous studies, we considered a large range of temperatures and colour excesses (and hence luminosities), both of which have been consistent with the spectral type. We have, however, assumed a mean Galactic extinction curve in calculating the extinction. The model is very dependent on the extinction curve as this affects the relative offsets of the light curves in different passbands. If the extinction curve were incorrect, then the fitting procedure would compensate for this by choosing different values for the distance, temperature and $E(B - V)$. Our temperature and $E(B - V)$ are in good agreement with the ‘observed’ spectral type, which implies that the actual extinction cannot significantly deviate from the mean Galactic curve. The greatest variations in Galactic extinction occur in the UV (Fitzpatrick 1999). Since our fits do not rely on UV data, we suspect that deviations from the Galactic mean are unlikely

to be important. The alternative to using the mean Galactic extinction curve would have been to shift the light curves in the modelling. However, as discussed previously, shifting the light curves arbitrarily is not desirable (since this leads to the loss of information) and so using the mean Galactic extinction curve is preferable, especially as the modelling proves to be fully self-consistent.

3.3.2 Modelling the disc

Our disc model is rather simple. For example, we assumed a flat cylindrical disc; this is unrealistic as the disc will almost certainly be more complicated with well defined structure. Possible evidence of structure can be seen in the *I* band data near phase 0.85 where there is a systematic offset between the data points and the light curve. The data points are dimmer with flux variations of up to 2.5 per cent. Even though the disc in our model contributes only a small fraction of the total flux (~ 5 per cent in *V*), the model is sensitive to its contribution (as can be seen from the comparison of the best-fitting models for different disc structures in Tables 2 and 3). In our modelling, we varied the size, temperature and power-law index of the disc. The size of the disc determines the depth of the grazing eclipse and hence the inclination. Since we varied these key disc parameters over a wide range of plausible values, we expect our estimates of the model parameters (e.g. the inclination and the component masses) and their uncertainties to be reasonably realistic.

The proportion of flux, the cool accretion discs in our models contribute to the total flux, increases with wavelength i.e. the minimum contamination is in *B*. This is different from models for the SXT A0620–00 (V616 Mon) where the disc contribution appears to decrease from 43 ± 6 per cent in *V* (Oke 1977; McClintock & Remillard 1986) to less than 27 per cent in the infrared (Shahbaz, Bandyopadhyay & Charles 1999). This shows that even in A0620–00, which has a much shorter orbital period (7.75 hr; McClintock & Remillard 1986) and has been in quiescence for much longer, the disc contributes appreciably to the total flux of the system.

On the other hand, Greene et al. (2001) have justified the use of a model without a disc by claiming that an accretion-disc model does not fit the data well and that the flux contribution from it will be negligible. The disc model they consider, however, contributes a large proportion of the *K* flux, as evidenced by the eclipses in their accretion-disc model at phase 0.0 as opposed to phase 0.5 for eclipses of the secondary. A model with a smaller proportion of *K* flux would have a larger amplitude than their accretion-disc model. This would better fit the data, decreasing the requirement for a model without an accretion disc. In the next section we will show that models without an accretion disc affect other model parameters, in particular the inferred distance, and that no fully self-consistent models can be obtained without a disc.

3.3.3 *J* and *K* magnitudes

Our model can also be used to make predictions for other passbands. Using our best-fitting models, we calculated the expected *J* and *K* band light curves. For the *J* and *K* bands

we find mean magnitudes of 13.8 and 13.0, respectively, with the disc contributing between 10 and 20 per cent of the total flux depending on the model. Greene et al. (2001) have recently presented *BVIJK* photometry of GRO J1655–40 in quiescence. They find mean *J* and *K* magnitudes of 13.85 and 13.25, respectively. Our *J* band prediction is in good agreement with their photometry apart from the depth of the minima, which is somewhat too low (possibly because the inclination is slightly too low). However, the general agreement in the *J* band provides some direct confirmation that the luminosity and colour excess found in our modelling are accurate. The amplitude of our *K* band light curve is also in good agreement with their photometry. We find a slightly larger amplitude than their best-fitting model but entirely consistent with their data. The reason for the *K* band mean magnitude discrepancy is not clear, although we have only calculated the best-fitting models and so do not know what range of *K* magnitudes is represented by our range of parameters.

Johnson (1966) provides intrinsic infrared colours for luminosity classes III and V. We may compare these to the colour implied by the photometry of Greene et al. (2001). Their *J* – *K* colour is 0.6. Assuming the standard *J* and *K* extinction coefficients of Fitzpatrick (1999), i.e. $(J - K)_0 = (J - K) - 0.5E(B - V)$, and our $E(B - V)$ of 1.0 ± 0.1 , we obtain a $(J - K)_0$ of 0.1 ± 0.05 . For luminosity class III, Johnson (1966) only lists the infrared colours for spectral type G5 and later. For luminosity class V, Johnson (1966) gives $(J - K)_0$ colours of 0.28 and 0.32 for spectral type F5 and G0, respectively – a $(J - K)_0$ colour of 0.1 would correspond to an A star. The $(J - K)_0$ colour appropriate for a F5 or G0 star would require a *J* – *K* of 0.8, similar to the value in our model. Hence there appears to be a deficit of *K* flux in the system, the cause of which is not clear.

We can easily check whether a similar discrepancy exists in the modelling of Greene et al. (2001). Using the parameters found in their modelling, we calculated how much their light curves have been shifted in each passband and determined the implied $E(B - V)$ and distance in their model. Using the shifts in all five bands, we find an $E(B - V)$ of 1.041 ± 0.022 and a distance of 4.008 ± 0.045 kpc. For this fit, however, the mean magnitudes in the different passbands are not in reasonable agreement with the data, mainly because of the inclusion of the *K* band. If we repeat the analysis without using the *K* band, we find an $E(B - V)$ of 1.076 ± 0.003 and a distance of 3.805 ± 0.013 kpc. This provides good agreement with the mean *B*, *V*, *I* and *J* magnitudes but produces a mean *K* magnitude of 13.06. Hence the discrepancy in the *K* band is present in their modelling as well. We also note that the implied distance in their model is substantially larger than that found from the kinematics of the radio jet. The reason is that their secondary is too massive and hence too luminous, requiring the system to be more distant in order to have the correct visual magnitude.

We ran our model without an accretion disc to see if a self-consistent model could be obtained in this way when fitting to the *B*, *V*, *R* and *I* data. We found a $\chi^2_{\nu, \min}$ of 3.120, substantially larger than the models with the accretion discs. Table 5 shows the best-fitting parameters for this case and the best-fitting values of Greene et al. (2001) who assumed a fixed effective temperature and who did not consider the distance or colour excess in calculating their light curves (the

Table 5. Best-fitting parameters for a self-consistent model without a disc compared to the results of Greene et al. (2001).

Parameter	Model	
	Self-consistent	Greene et al. (2001)
Mass ratio	2.4	2.6 ± 0.3
Inclination	$77^\circ.7$	$70^\circ.2 \pm 1^\circ.9$
$E(B - V)$	1.127	1.076^1
Distance (kpc)	3.712	3.805^1
T_{pole} (K)	6950	6768
Minimum χ^2_{ν}	3.118	1.612
M_1 (M_{\odot})	5.9	6.3 ± 0.5
M_2 (M_{\odot})	2.4	2.4 ± 0.4
L_2 (L_{\odot})	40.1	31.9–40.6
T_{eff} (K)	6500	6336 (Fixed)

¹Implied from their data (see Section 3.3.3).

values shown are those implied by their model as described above).

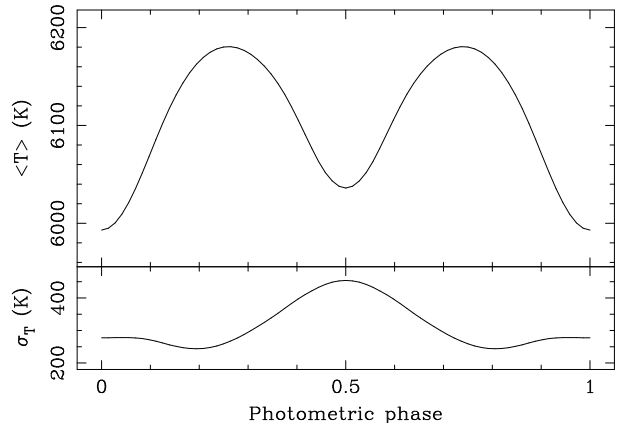
It is clear that the secondary in our model is similar to the secondary in their model, with a similar mass, temperature and luminosity. We find, however, a higher inclination. This is due to the higher temperature of the secondary which is correlated with the inclination. We note, however, that the secondary is similar and that in eclipsing systems there is a strong constraint on the inclination due to the depth of the eclipse. Hence, we can be satisfied that both the inclination and the other system parameters are accurate in the previous models. The lower mass ratio is clearly a consequence of neglecting the accretion disc.

Due to the large χ^2_{ν} of the model without an accretion disc, we therefore conclude that an accretion is required for any self-consistent model of Nova Sco.

4 THE VARIATION IN SURFACE TEMPERATURE AND IMPLICATIONS FOR THE DETERMINATION OF THE SPECTRAL TYPE

As a result of gravity darkening, there is a large variation in temperature across the surface of the secondary, and hence an observer will see a variation of the secondary’s temperature as a function of orbital phase. To determine the magnitude of this effect, a flux-weighted average temperature and its standard deviation were calculated at each orbital phase. For the flux-weighting we used the R band which has a wavelength range similar to that of the spectra previously used for the determination of the spectral type (6350–6750Å).

Fig. 3 shows the variation in average temperature and the standard deviation in the flux-weighted temperature distribution with phase for the best-fitting model parameters of Section 3. It demonstrates that the average ‘observed’ temperature of the secondary is substantially lower (~ 450 K) than the temperature at the poles where the gravity is largest. There is also a clear variation in average temperature with phase (~ 200 K). This variation would be large enough to change the observed spectral sub-type with phase if there was not such a large range of temperatures across

**Figure 3.** The variation in the flux-weighted average temperature and its standard deviation for the best-fitting model as a function of phase.

the observable part of the secondary at each phase. The total range within one standard deviation is 5600–6500 K. This range corresponds to stars of spectral sub-type F5–G5 (Straižys & Kuriliene 1981). The effect this variation in temperature has on the observed line profiles is unknown and is worth further investigation. We conclude, however, that it is difficult to determine the spectral type to better than a few sub-types due to this large variation in surface temperature.

5 DISCUSSION

5.1 Comparison to previous studies

The accretion-disc model with a flat temperature profile provides the best-fitting model. This result is consistent with disc structures in CVs during quiescence (based on MEM), which appear to have temperature profiles that are much flatter than those expected for steady-state discs. VdH found that, for a steady-state disc, there were no reasonable solutions with rim temperatures greater than 1000 K. This is consistent with our results as the models with a 2000 K disc do not provide good fits to the data unless the inner disc is removed. OB allowed the power-law exponent for the temperature profile, the rim temperature and the size of the disc to be free parameters. They obtained a best-fitting power-law exponent of -0.12 ± 0.01 , a rim temperature of 4317 ± 75 K and an outer disc radius of $0.747 r_L$. With an exponent of -0.1 , we fit the data with a disc rim temperature of 3500 K at $0.9 r_L$, which at the radius $0.747 r_L$ has a temperature of 3580 K. Hence the disc in this model is 750 K cooler than that found by OB. The accretion disc model with a central hole contributes predominantly red light as it has a low average temperature, similar to the disc with the flat temperature profile. Hence we can conclude that the disc in GRO J1655–40, when it is in quiescence, is predominantly red and cool. Although the flatter temperature profile is preferred in the modelling, the actual disc will almost certainly be more complicated.

OB only considered one accretion disc structure in their model, although their accretion-disc parameters were free to vary. Our analysis shows that the system parameters vary with the accretion-disc model. Hence, a range of accretion-

disc models need to be considered in order to avoid underestimating the systematic errors. Relying on the minimization of χ^2 is insufficient as the modelling is not sufficiently accurate to enable a reliable determination of the precise accretion-disc structure. This is because, as mentioned earlier, the actual accretion-disc will be more complicated than the simple model assumed in these analyses.

Indeed, from our analysis, it is clear that a large range of mass ratios and hence masses will fit the light-curve amplitudes. These amplitudes are strongly dependent on the accretion-disc model and the proportion of flux for each model in each band. GRO J1655–40 has a secondary of earlier spectral type and hence higher luminosity than most other SXTs. This means that accretion-disc contamination is less important than in other systems, although it still strongly affects the inferred system parameters. We therefore used the independent distance determination from the kinematics of the radio jet (Hjellming & Rupen 1995), as used previously to model the jets in SS 433 (Hjellming & Johnston 1988) to further constrain the allowed disc models. There are, however, a number of possible systematic errors in this measurement. The inclination of the jet axis of $85^\circ \pm 2^\circ$ is significantly different from the system inclination of $68.65 \pm 1.5^\circ$, implying a more complicated geometry than the simple model they use. This model also does not describe all the structure observed in the jet, and there are deviations from simple linear expansion which they assume. In addition there is motion over the length of an observation which would result in smearing. On the other hand, they chose a beam-width larger than the proper motion during each six-hour VLBA observation to minimize this effect. These observations did not have absolute positional information resulting in the central source being used for reference. This is undesirable as it makes the alignment of the different images in their analysis a free parameter. If this distance measurement were incorrect, this could somewhat alter our best-fitting parameters. Distance estimates by other authors are, however, consistent with their determination: ~ 3 kpc (Bailyn et al. 1995a); ~ 3 kpc (Greiner, Predehl & Pohl 1995); 3.5 kpc (McKay & Kesteven 1994) and 3–5 kpc (Tingay et al. 1995). Hence, using their distance determination of 3.2 ± 0.2 kpc as additional constraint is reasonable.

A lower value for the colour excess than used previously is needed to provide good fits to the data in all passbands simultaneously. We found an $E(B - V)$ of 1.0 ± 0.1 (90 per cent confidence). This value is somewhat, but not dramatically lower than various previous estimates (1.15, Bailyn et al. 1995a; 1.3, Horne et al. 1996; 1.2 ± 0.1 , Hynes et al. 1998, 1σ limits). This $E(B - V)$ along with the effective temperature implies a spectral type range for the secondary of F5–G0, consistent with previous estimates (S99). VdH used a value for the colour excess of 1.3 in their study and hence had to assume a significantly larger luminosity of the secondary ($31 - 54 L_\odot$ as compared to $21.0 \pm 6.0 L_\odot$ found here). This resulted in significantly larger masses for both the black hole and the secondary. A lower luminosity, which alters GRO J1655–40’s position in the HR diagram, along with the lower masses implied by our model has implications for the interpretation of the system’s evolutionary state (see Section 5.3).

Mass estimates for the components have also been obtained by Buxton & Vennes (2001) and Wagoner, Silbergleit

& Ortega-Rodríguez (2001). Buxton & Vennes (2001) fitted model spectra to the observed quiescent spectrum and measured the rotational broadening in order to calculate a mass ratio of 2.56–4.35 using the radial velocity amplitude of S99 (see Section 5.2). Combined with the inclination of vdH the masses are $7.91 \pm 3.79 M_\odot$ and $2.76 \pm 1.79 M_\odot$ for the primary and secondary respectively. Wagoner et al. (2001) have modelled the quasi-periodic X-ray oscillations and find a primary mass of $5.9 \pm 1.0 M_\odot$. Both of these measurements are consistent with our values.

5.2 Rotational broadening and the mass ratio

Our mass ratio of 3.9 ± 0.6 is larger than that found in the study of OB (2.60–3.45, 3σ limits) but is in agreement with the upper range obtained by vdH (2.43–3.99, 3σ). A larger mass ratio implies a smaller and hence less luminous secondary, as required by our lower value for the colour excess. S99 found a mass ratio of 2.29–3.06 (95 per cent confidence) based on their estimate of the rotational broadening of the spectral lines. They assumed that the secondary was spherical and that all the observed broadening was a consequence of rotation. Fitting a broadening profile to template star spectra and minimizing the residuals, they found a rotational velocity, $v \sin i$, of $82.9 - 94.9 \text{ km s}^{-1}$. Our mass ratio range corresponds to a $v \sin i$ of $68.3 - 79.1 \text{ km s}^{-1}$, using their broadening to mass ratio relation. In their determination of the average spectrum, S99 did not correct for the orbital smearing of the spectra due to the length of the exposure time of the observations. Most of their spectra were taken near the quadrature phases when orbital smearing would be at its greatest. This results in the apparent broadening of the lines by 7 km s^{-1} (at the orbital phase when the spectra were taken). Since this broadening should be added linearly to the rotational broadening (rather than in quadrature), it introduces an additional, but spurious rotational broadening of 3.5 km s^{-1} (about half of the change of the radial velocity during the observations).

S99 took the radius of a spherical star in their model to be the effective Roche-lobe radius. In reality, a Roche-lobe filling object can be described by an ellipsoid to first approximation. This implies that the light contributing to a spectral line will come from a larger range of radii (and hence velocities) than for a spherical star of the same volume and that the assumption of sphericity will lead to an overestimate of the rotational velocity. The dependence of $v \sin i$ on the mass ratio for a realistic model containing a Roche-lobe filling star is consequently non-trivial and requires detailed modelling. Orosz & Hauschildt (2000) have investigated the difference in rotational broadening kernels between Roche-lobe filling models and analytical models. They found that, for a Roche-lobe filling star, the broadening kernel changes with phase and is significantly different near the quadrature phases where it is wider and asymmetric. The calculation using the analytical kernel then provides an upper limit to $v \sin i$. Since an upper limit on the rotational broadening provides a lower limit to the mass ratio, we conclude that our estimates are likely to be consistent with the findings of S99, once all of these effects are properly taken into account.

Greene et al. (2001) calculated a numerical broadening kernel for photometric phase zero, where the Israelian et al. (1999) measurements were taken. They found almost

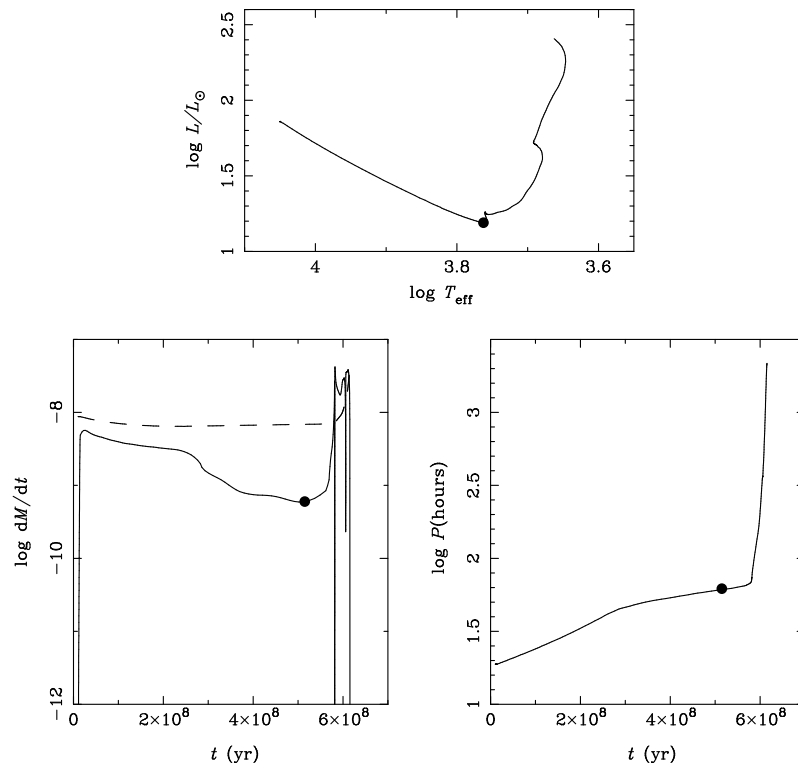


Figure 4. Binary evolution model for Nova Sco (conservative case A mass transfer with convective overshooting of 0.3 pressure scale heights). The individual panels show the Hertzsprung-Russell diagram, the mass-transfer rate and orbital period since the beginning of mass transfer. The evolution after mass transfer has ceased is not shown. The initial masses of the black hole and secondary are 4.1 and $2.5 M_{\odot}$, respectively, the present masses are 5.3 and $1.3 M_{\odot}$. The secondary is close to exhausting hydrogen in its core. The dots indicate the values at the orbital period of Nova Sco (2.6 d). The dashed curve in the \dot{M} panel shows the critical mass-transfer rate below which transient behaviour is expected (from King, Kolb, & Szuskiwicz 1997).

no systematic biases in comparison to the analytical kernel, justifying the use of $v \sin i$ of $93 \pm 3 \text{ km s}^{-1}$ in their model fitting. Buxton & Vennes (2001) have calculated $v \sin i$ by fitting model spectra to the observed spectrum taken during quiescence and found a $v \sin i$ of $80 \pm 10 \text{ km s}^{-1}$ as well as $T_{\text{eff}} = 6500 \pm 50 \text{ K}$ and $[\text{Fe}/\text{H}] = -0.25 - 0.00$. This is consistent with our calculation as well as with previous measurements. Their Fe abundance agrees with that of Israelian et al. (1999) who found $[\text{Fe}/\text{H}] = 0.1 \pm 0.2$ and larger overabundances in α -process elements. Recently, Bleach et al. (2000) have demonstrated the unreliability of using the rotational broadening $v \sin i$ for the calculation of system parameters in the CV EG Uma. They fitted broadened spectra to individual lines and found a large range of values of $v \sin i$ of $19 - 59 \text{ km s}^{-1}$, with typical error on each value of $\sim 10 \text{ km s}^{-1}$. As the velocity semi-amplitude of both components in this system is measurable, they predict a $v \sin i$ of 28.6 km s^{-1} . The reason for this large variation is unknown, but is not due to irradiation and may be a result of anomalous composition (for further discussion see Wood et al. 2001).

5.3 The evolutionary state of GRO J1655–40

Modelling the binary evolution of GRO J1655–40 with a present secondary mass of $2.35 M_{\odot}$ (OB) leads to an average (secular) mass-transfer rate that tend to be much larger than is consistent with its X-ray transient behaviour (van

Paradijs 1996; King, Kolb & Szuskiwicz 1997). Kolb et al. (1997) and Kolb (1998) showed that this problem could be solved if the secondary were in a special position in the Hertzsprung gap; this, however, required a somewhat cooler secondary than is consistent with its spectral type. Regós, Tout & Wickramasinghe (1998) suggested as an alternative solution that the secondary is still on the main sequence. This also requires some fine-tuning and significant convective overshooting (but is consistent with recent findings; Pols et al. 1997).

The lower mass found in this re-analysis largely removes this problem, irrespective of whether the secondary is still on the main sequence or in the Hertzsprung gap. To illustrate this we present a case A binary calculation (similar to the model of Regós et al. 1998) in Fig. 4 (for a detailed description of the binary evolution code see Podsiadlowski, Rappaport & Pfahl 2001a). The dashed curve in the panel showing the mass-transfer rate gives the critical mass-transfer rate below which transient behaviour is expected (from King et al. 1997). The mass-transfer rate is well below the critical rate until the end of the main sequence. We have also performed some early case B binary calculations (i.e. where the secondary has just evolved off the main sequence) and also find that, with the lower mass of the secondary, the present mass-transfer rate is below the critical rate for transient behaviour, although case B models generally do not fit as well as late case A models.

In our case A model, the initial masses, i.e. immediately after the supernova in which the black hole was formed, were 4.1 and $2.5 M_{\odot}$ for the black hole and secondary, respectively. These masses are very similar to the post-supernova masses required to explain the pollution of the secondary with α -process material (Israelian et al. 1999) that was ejected in the supernova (Podsiadlowski et al. 2001b)².

From all of this a complete picture starts to emerge for the evolutionary history of Nova Sco. The pollution of the secondary with supernova material proves that the black hole formed in a supernova (or a hypernova). Some material that was produced in the supernova had to be captured by the secondary; this requires both fallback of material and mixing in the supernova ejecta (Podsiadlowski et al. 2001b). In a typical model, the orbital period after the binary has re-circularized after the supernova is about 20 hr (see the mixing models in table 3 of Podsiadlowski et al. 2001b), very close to the period needed for a late case A scenario as shown in Fig. 4. Since then the secondary has transferred some $1 M_{\odot}$, increasing the orbital period to its present value. Self-consistent models also require that the black hole received a significant kick at birth in order to produce the high observed system space velocity, consistent with the fallback suggestion by Brandt, Podsiadlowski & Sigurdsson (1995).

6 CONCLUSIONS

We have obtained self-consistent fits to the ellipsoidal light curves of GRO J1655–40 for the B , V , R and I passbands simultaneously without making *a priori* assumptions about the distance and the colour excess. Using the distance estimate of 3.2 ± 0.2 kpc, based on the kinematics of the radio jet, as additional constraint, we find that our $E(B - V)$ of 1.0 ± 0.1 along with our effective temperature of the secondary of 6150 ± 350 K corresponds to a spectral type range for the secondary of F5–G0. This is consistent with the spectral type found by S99. Our mass ratio, larger than found previously, of 3.9 ± 0.6 , along with our inclination of $68.65 \pm 1.5^{\circ}$ implies lower masses of $5.4 \pm 0.3 M_{\odot}$ and $1.45 \pm 0.35 M_{\odot}$ for the black hole and the companion, respectively. The mass ratio along with the $E(B - V)$ also implies a lower luminosity of the secondary of $21.0 \pm 6.0 L_{\odot}$. These results are, however, rather sensitive to the assumptions about the disc structure (even though in V the disc only contributes some 5 per cent of the light). Our best-fitting models have a disc temperature profile that is much flatter than that of a steady-state disc. The reduced revised masses also help to explain the transient nature of the system

² We note that, in order to explain its anomalous composition, the secondary had to capture some $0.25 M_{\odot}$ of material mainly composed of heavy elements, which was then mixed completely with the secondary (Podsiadlowski et al. 2001b). This must have dramatically changed the composition (in particular the metallicity) of the secondary, an effect that was not included in our binary calculations.

ACKNOWLEDGEMENTS

We thank Jerry Orosz for kindly providing the light-curve data which has made this analysis possible. MEB thanks Tariq Shahbaz and Janet Wood for useful discussion.

REFERENCES

- Avni Y., 1976, ApJ, 210, 642
 Bailyn C. D. et al., 1995a, Nat, 374, 701
 Bailyn C. D., Orosz J. A., McClintock J. E., Remillard R. A., 1995b, Nat, 378, 157
 Bessell M. S., 1990, PASP, 102, 1181
 Bleach J. N., Wood J. H., Catalán M. S., Welsh W. F., Robinson E. L., Skidmore W., 2000, MNRAS, 312, 70
 Brandt W. N., Podsiadlowski Ph., Sigurdsson S., 1995, MNRAS, 277, L35
 Buxton M., Vennes S., 2001, PASA, 18 (1), 91
 Fitzgerald M. P., 1970, A&A, 4, 234
 Fitzpatrick E. L., 1999, PASP, 111, 63
 Greene J., Bailyn C. D., Orosz J. A., 2001, ApJ, 554, 1290
 Greiner J., Predehl P., Pohl M., 1995, A&A, 297, L67
 Hameury J. M., Lasota J. P., McClintock J. E., Narayan R., 1997, ApJ, 489, 234
 Hjellming R. M., Johnston K. J., 1988, ApJ, 328, 600
 Hjellming R. M., Rupen M. P., 1995, Nat, 375, 464
 Horne K., 1993, in Wheeler J. C., ed., Accretion disks in compact stellar systems. World Scientific Publishing Company, Singapore, p. 117
 Horne K. et al., 1996, IAU Circ. 6406
 Hynes R. I. et al., 1998, MNRAS, 300, 64
 Israelian G. et al., 1999, Nat, 401, 142
 Johnson H. L., 1966, ARA&A, 4, 193
 King A. R., Kolb U., Szuszkiewicz E., 1997, ApJ, 488, 89
 Kolb U., 1998, MNRAS, 297, 419
 Kolb U., King A. R., Ritter H., Frank J., 1997, ApJ, 485, L33
 Kurucz R. L., 1992, Rev. Mex. Astron. Astrophys. 23, 181
 Lucy L. B., 1967, Z. Astrophysik, 65, 89
 McClintock J. E., Remillard R. A., 1986, ApJ, 308, 110
 McKay D., Kesteven M., 1994, IAU Circ. 6062
 Meyer F., Meyer-Hofmeister E., 1994, A&A, 288, 175
 Meyer-Hofmeister E., Meyer F., 2000, A&A, 355, 1073
 Narayan R., McClintock J. E., Yi I., 1996, ApJ, 451, 821
 Oke J. B., 1977, ApJ, 217, 181
 Orosz J. A., Bailyn C. D., 1997, ApJ, 477, 876 (OB)
 Orosz J. A., Hauschildt P. H., 2000, A&A, 364, 265
 Phillips S. N., Shahbaz T., Podsiadlowski Ph., 1999, MNRAS, 304, 839
 Podsiadlowski Ph., Rappaport S., Pfahl E., 2001a, ApJ, submitted
 Podsiadlowski Ph., Nomoto K., Maeda K., Nakamura T., Mazzali P., Schmidt B., 2001b, ApJ, submitted
 Pols O. R., Tout C. A., Schröder K., Eggleton P. P., Manners J., 1997, MNRAS, 289, 869
 Regős E., Tout C. A., Wickramasinghe D., 1998, ApJ, 509, 362
 Shahbaz T., van der Hooft F., Casares J., Charles P. A., van Paradijs J., 1999, MNRAS, 306, 89 (S99)
 Shahbaz T., Bandyopadhyay R. M., Charles P. A., 1999, A&A, 346, 82
 Shakura I. N., Sunyaev R. A., 1973, A&A, 24, 337
 Straizys V., Kuriliene G., 1981, Ap&SS, 80, 353
 Tingay S. J. et al., 1995, Nat. 374, 101
 Tüg H., White N. M., Lockwood G. W., 1977, A&A, 61, 679
 van der Hooft F., Heemskerck M. H. M., Alberts F., van Paradijs J., 1998, A&A, 329, 538 (vdH)
 van Paradijs J., 1996, ApJ, 464, L139
 von Zeipel H., 1924, MNRAS, 84, 665

- Wade R. A., Rucinski S. M., 1985, *A&AS*, 60, 471
- Wagoner R. V., Silbergleit A. S., Ortega-Rodríguez M., 2001, *ApJL* submitted (astro-ph/0107168)
- Wood J. H., Horne K., Berriman G., Wade R., O'Donoghue D., Warner B., 1986, *MNRAS*, 219, 629
- Wood J. H., Horne K., Berriman G., Wade R., 1989, *ApJ*, 341, 974
- Wood J. H., Bleach J. N., Catalán M. S., Welsh W. F., Robinson E. L., 2001, in Podsiadlowski Ph., Rappaport S., King A. R., D'Antona F., Burderi L., eds, *ASP Conf. Ser. Vol. 229, Evolution of Binary and Multiple Star Systems*. Astron. Soc. Pac., San Francisco, p. 267

This paper has been typeset from a $\text{T}_{\text{E}}\text{X}/\text{L}^{\text{A}}\text{T}_{\text{E}}\text{X}$ file prepared by the author.